Physica Scripta

PAPER

Enhancing the excitation of a high-index nanowire by adding a flat-ended head

To cite this article: Song Zhou and Wenchao Zhou 2022 *Phys. Scr.* **97** 085505

View the article online for updates and enhancements.

You may also like

- Interplay between entanglement and entropy in two-qubit systems
L Mazzola, S Maniscalco, J Piilo et al.
- Facile modification of freestanding silicon nitride microcantilever beams by dry film photoresist lithography
Madeleine Nilsen, Fabian Port, Michael Roos et al.
- Indentation responses of piezoelectric layered half-space
Y F Wu, H Y Yu and W Q Chen

This content was downloaded from IP address 159.226.165.22 on 07/02/2023 at 01:04

Physica Scripta

PAPER

Enhancing the excitation of a high-index nanowire by adding a flat-ended head

RECEIVED
14 April 2022

REVISED
27 June 2022

ACCEPTED FOR PUBLICATION
6 July 2022

PUBLISHED
15 July 2022

Song Zhou[1,*] **and Wenchao Zhou**[2]

[1] Jiangsu Key Laboratory of Advanced Manufacturing Technology, Faculty of Mechanical and Material Engineering, Huaiyin Institute of Technology, Huai'an 223003, People's Republic of China
[2] State Key Laboratory of Applied Optics, Changchun Institute of Optics, Fine Mechanics and Physics, Chinese Academy of Sciences, Changchun 130033, People's Republic of China
[*] Author to whom any correspondence should be addressed.

E-mail: zs41080218@126.com **and** zhouvc@ciomp.ac.cn

Keywords: high-index nanowire, enhanced excitation, flat-ended head

Abstract

A method for enhancing the excitation of a high-index nanowire with an added flat-ended head is numerically investigated. With the assistant of a flat-ended head, the intensity and the power flow of the high-index nanowire illuminated under a plane wave can be both enhanced. Our simulation shows that the enhancement factor is influenced by the length and the refractive index of the nanowire, and the size of the flat-ended head. The enhanced excitation of a silicon nanowire under a near-infrared illumination by an added flat-ended head is studied. Finally, the enhanced excitation affected by the incident angle is discussed.

1. Introduction

In the past several decades, nanowires have attracted considerable interest in nanotechnology [1–3]. Their cross-sectional dimensions are tens to hundreds of nanometers and length is typically micrometers. Due to the high large surface-to-volume ratio, nanowires can lead to strongly enhanced surface effects as compared to bulk materials in optics [4]. This optical surface fields can be used in nanoscale biomolecules sorting and sensoring [5–9]. For the liquid surroundings, high-index nanowires should be employed to produce the evanescent fields. High intensity excitation of the nanowire is important for improving the efficiency of optical sorting and sensoring.

Recently years, a photonic nanojet with high intensity and narrow beam waist produced by a microsphere or microcylinder has attracted lots of interests [10–13]. In [14], it showed that the structure supporting the photonic nanojet had a high numerical aperture. Besides, it was showed that the dielectric microsphere with low-numerical aperture could replace the 1.4 numerical aperture oil objective for quantum dot imaging in [15]. Considering free space light guided by a lens with a high numerical aperture into a fiber, the structure supporting the photonic nanojet can be used for the guidance of free space light into waveguides. On the other side, high-index structures can produce an ultra-narrow photonic nanojet, such as an engineered two-layer microcylinder of high refractive index materials [16], a truncated high-index cylinder [17], and a high-index flat-ended cylinder [18, 19].

In this paper, we present a method for enhancing the excitation of high-index nanowires by adding a flat-ended head. At first, the enhanced excitation of the high-index nanowire is investigated by adding a circle head and a flat-ended head. Then, the enhancement factor of the power flow of the nanowires influenced by the length and the refractive index of the nanowires, and the size of the flat-ended head are studied. And the enhanced excitation of a silicon nanowire by adding a designed flat-ended head under 1550 nm illumination is presented. Finally, we study the influences of the incident angle on the enhanced excitation of the silicon nanowire with the designed head.

© 2022 IOP Publishing Ltd

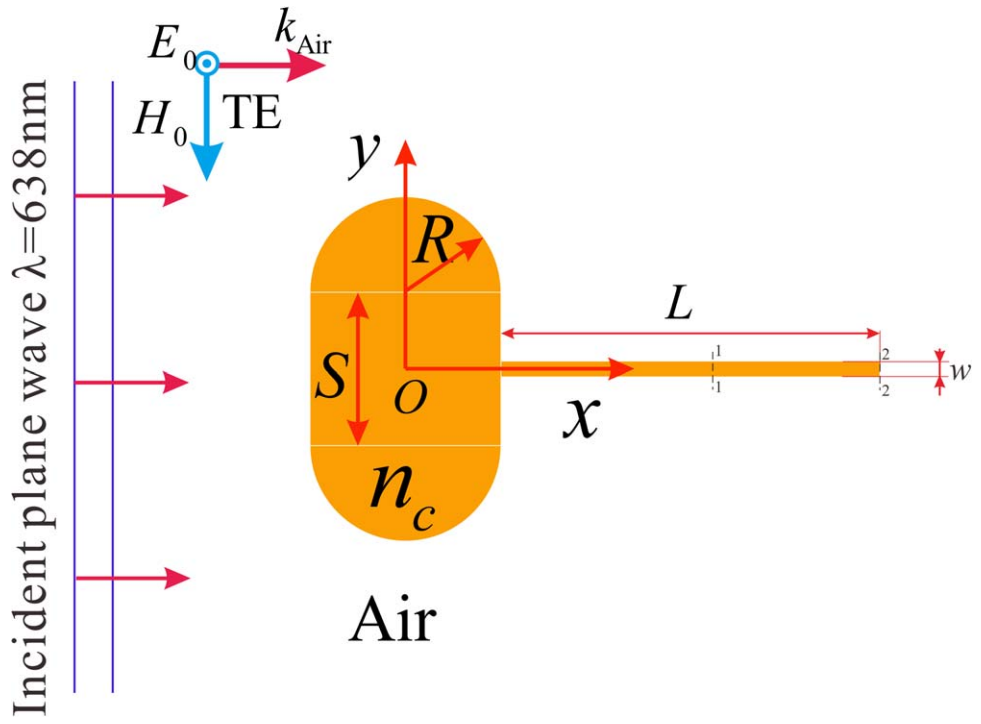

Figure 1. Schematic of the model: a nanowire with a flat-ended head illuminated by a plane wave.

2. Models and methods

For reducing the computational complexity, a 2D model is adopted in the wave optics module of CMOSOL Multiphysics [20], a commercial finite element software. As shown in figure 1, the incident wave is a plane wave propagating along positive x direction, while its electric filed is chosen as TE-polarization. For the flat-ended head, it includes two round heads with the radius R and one flat body with the length S. A nanowire is put at the shadow of the flat-ended head with the length set to L and the width chosen as w. Two cross sections are selected for detecting the power propagating along positive x direction. One cross section at right side 500 nm of the center of the nanowire is marked as 1–1, and the other cross section at the right end of the nanowire is marked as 2–2. The refractive index of the head and the nanowire is set to n_c, and they are put in air with the refractive index set to 1. The TE-polarized plane wave, with a wavelength of $\lambda = 638$ nm and intensity $E_0 = 1$, is added into the wave module as a background field. In order to obtain the computational validity, the perfectly matched layer absorbing boundary conditions are used around the simulated domain. To achieve simulation accuracy, the maximum element size of the free triangular mesh is chosen as 20 nm in the full domain. The intensity in this paper is defined as the full electric field squared.

3. Results and discussions

At first, we investigate the enhanced excitation of a nanowire by adding a flat-ended head. The results are shown in figure 2. In our simulation, a nanowire with $n_c = 3$, $L = 10$ μm and $w = 100$ nm is selected. Two kinds of heads are utilized, a circle one with the radius $R = 1$ μm and a flat-ended one with the round radius $R = 1$ μm and the body length $S = 500$ nm. Intensity distributions are shown in figure 2(a) for the single nanowire, in figure 2(b) for the nanowire with a circle head and in figure 2(c) for the nanowire with a flat-ended head. In order to clearly show the results, insert pictures picked out from the red dotted box are enlarged in figures 2(a), (b) and (c), respectively. The detailed information of intensity distribution and power flow inside of the red dotted box along x direction (P_x) at the nanowire center is shown in figures 2(d) and (e), respectively. By comparison, the excitation of the nanowire is enhanced by adding a circle head or a flat-ended head. In figure 2(d), it shows that the maximum intensity enhancement factor can reach about 5 times than that of a single nanowire by adding a circle head, while the maximum intensity enhancement factor is about 8 times for the flat-ended head. For P_x, the flat-ended head can make the enhancement factor reaching nearly 7 times shown in figure 2(e). The results in figure 2 demonstrate that the flat-ended head is effective in enhancing the excitation of the nanowire.

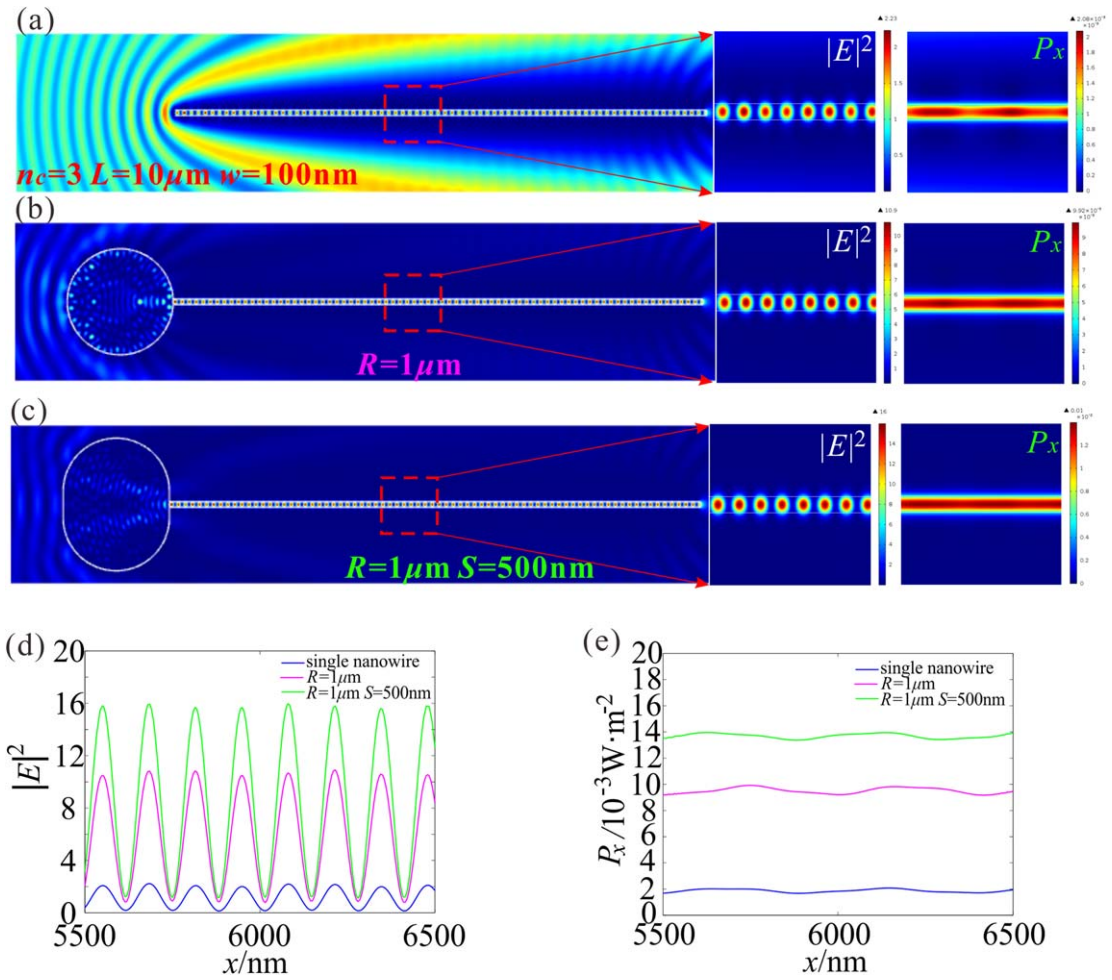

Figure 2. (a) A high-index nanowire with $n_c = 3$, $L = 10$ μm and $w = 100$ nm excited by a TE-polarized plane wave, (b) enhancing the excitation of the nanowire in (a) by adding a circle head with the radius $R = 1$ μm, (c) enhancing the excitation of the nanowire in (a) by adding a flat-ended head with the round radius $R = 1$ μm and the body length $S = 500$ nm, the two insert pictures for intensity and power flow along x direction (P_x) in (a), (b) and (c) are the enlarged views inside of the red dotted box, respectively. The detailed information inside of the red dotted box along x direction at the nanowire center is presented in (d) for intensity distributions and in (e) for power flow, respectively.

In the following part, the excitation of the nanowire with a flat-ended head influenced by the refractive index n_c and the length L of the nanowire, and the flat body length S is studied. In figure 3, the flat-ended heads with $R = 1$ μm and four kinds of the body length S are adopted to improve the excitation of the nanowire with $n_c = 3$, $w = 100$ nm and the length L ranging from 9 to 11 μm with a step set to 100 nm. We use the power propagating inside the nanowire to evaluate the enhancement. The power is the integration of P_x along the detected cross sections 1–1 or 2–2 shown in figure 1. The power propagating inside of the nanowire as a function of the nanowire length at the 1–1 cross section is given in figure 3(a), the left picture shows the power and the right picture presents the power ratio, which is defined as the power inside the nanowire with a head divided by the power inside the single nanowire. In figure 3(b), it is shown the results detected at the 2–2 cross section. Intensity distribution and P_x of the flat-ended with $S = 400$ nm and $R = 1$ μm and the nanowire length $L = 10$ μm are simulated and the results picked out from the red dotted line same as that in figure 2(a) are shown in figure 3(c). In figures 3(a) and (b), the power of a single nanowire excited under a plane wave is fluctuant as the change of the length L, and the size of the added head can affect the power enhancement factor. It can be seen that the flat-ended head with the body length $S = 400$ nm has the maximum power value, while the flat-ended head with $S = 300$ nm has the maximum power ratio value of the nanowire in the results shown in figures 3(a) and (b). In figure 3(c), it is indicated that the intensity enhancement factor reaches more than 10 times of the single nanowire in figure 2(a). From the results in figure 3, it is shown that optimizing the body length S and the length L of the nanowire with an added flat-ended head can achieve high excitation. In figure 4, we investigate the influence of the refractive index n_c on the excitation. Power propagating inside of the nanowire as a function of the nanowire length at the 1–1 cross section is shown in figure 4(a) for the refractive index $n_c = 2.5$ and figure 4(b) for the refractive index $n_c = 3.5$, respectively. The power of the nanowire with the refractive index

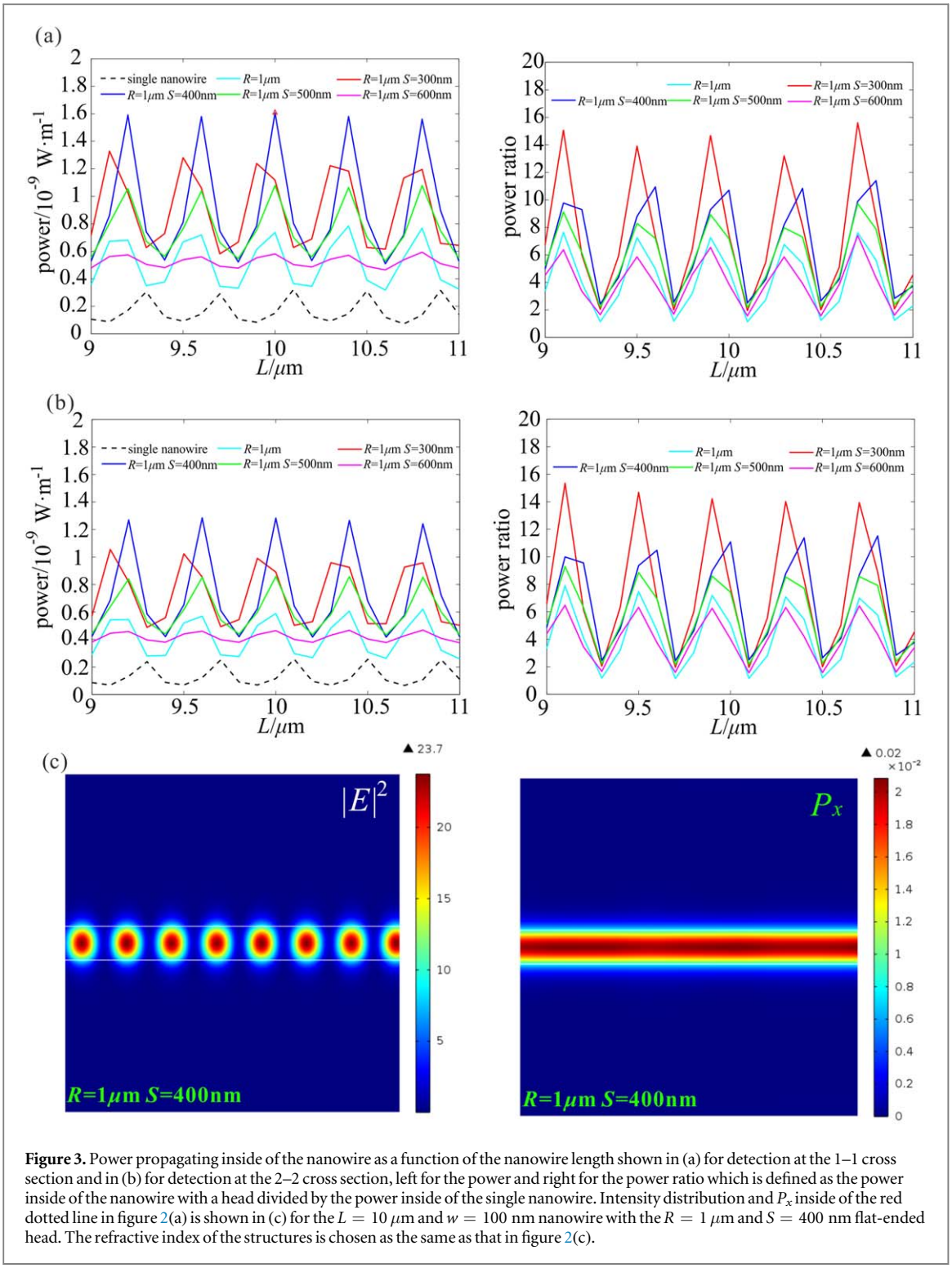

Figure 3. Power propagating inside of the nanowire as a function of the nanowire length shown in (a) for detection at the 1–1 cross section and in (b) for detection at the 2–2 cross section, left for the power and right for the power ratio which is defined as the power inside of the nanowire with a head divided by the power inside of the single nanowire. Intensity distribution and P_x inside of the red dotted line in figure 2(a) is shown in (c) for the $L = 10$ μm and $w = 100$ nm nanowire with the $R = 1$ μm and $S = 400$ nm flat-ended head. The refractive index of the structures is chosen as the same as that in figure 2(c).

$n_c = 2.5$ is fluctuant similar to that shown in figure 3(a), while it becomes more subdued than that in figure 4(a) when the refractive index is selected as $n_c = 3.5$. For $n_c = 2.5$, the flat-ended head with the body length $S = 300$ nm can provide high excitation of the nanowire, while $S = 300$ nm and $S = 400$ nm are both suited for $n_c = 3.5$. This result means that the enhanced excitation by adding a flat-ended head may be valid for a silicon nanowire at a near-infrared illumination.

The enhanced excitation of a silicon nanowire by adding a designed flat-ended head under 1550 nm illumination is investigated. The results are given in figure 5. Considering the illumination wavelength, the refractive index of silicon medium is $n_c = 3.4777$ from [21]. A silicon nanowire with $w = 100$ nm is connected with a silicon flat-ended head with $R = 1$ μm and $S = 400$ nm at the shadow of the silicon nanowire. Power propagating inside of the silicon nanowire as a function of the nanowire length at the 1–1 cross section shown in figure 1 is provided in figure 5(a). The intensity of the structure picked out from figure 5(a) using a pink triangle

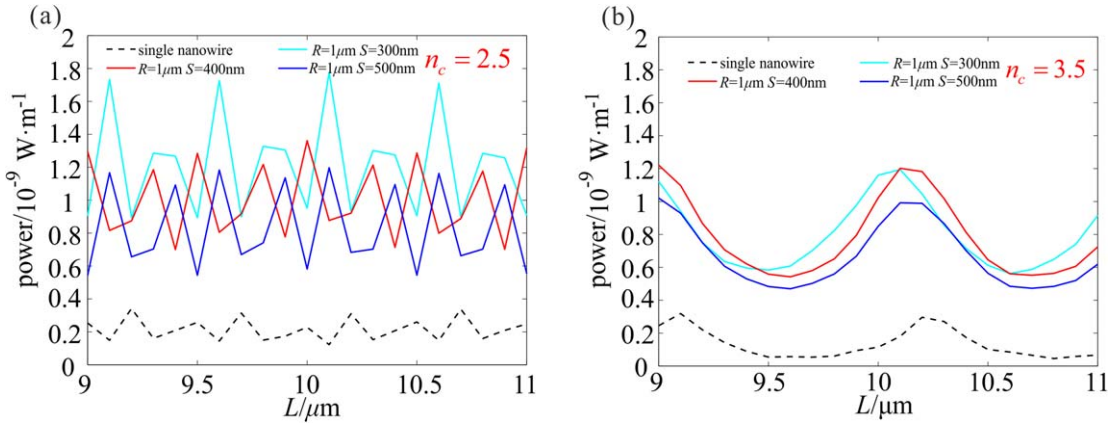

Figure 4. Power propagating inside of the nanowire as a function of the nanowire length at the 1–1 cross section provided in (a) for the refractive index $n_c = 2.5$ and (b) for the refractive index $n_c = 3.5$. The other parameters are the same as those in figure 2(c).

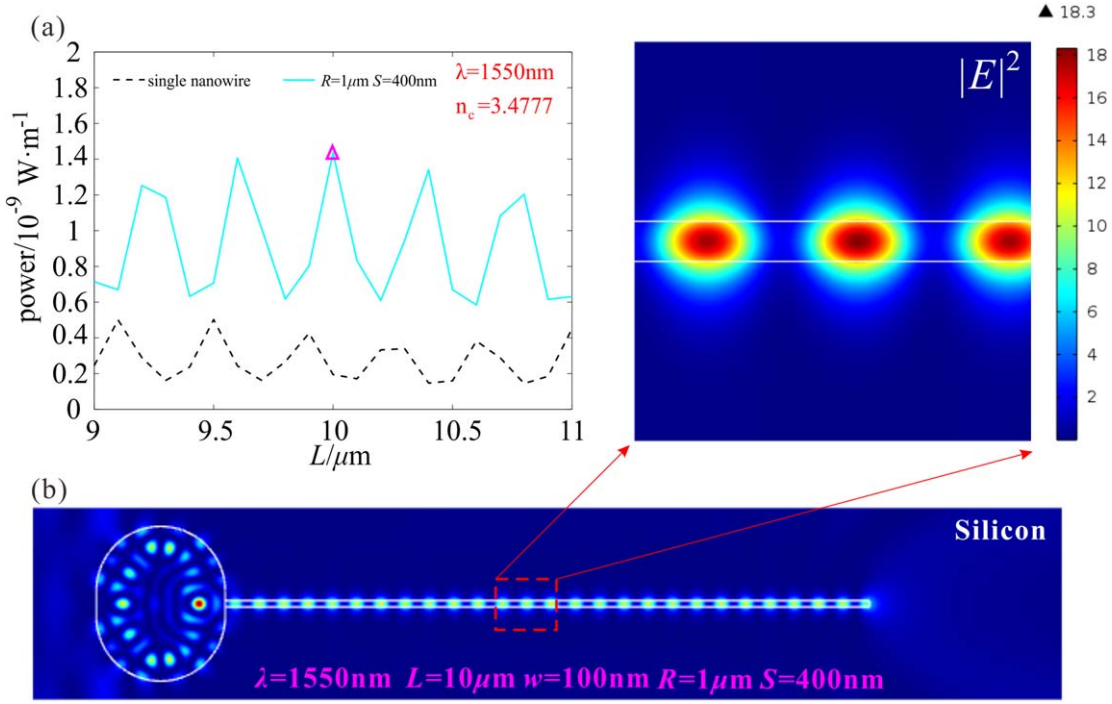

Figure 5. Excitation of a silicon nanowire enhanced using a flat-ended head. Power propagating inside of the nanowire as a function of the nanowire length at the 1–1 cross section shown in (a), while the intensity of the structure with the largest enhancement in simulation provided in (b).

marker is shown in figure 5(b). The intensity enhancement factor reaches 18.3 compared with the intensity of the incident wave. The results in figure 5 indicate the excitation of silicon nanowire can be improved by adding an appropriate flat-ended head.

Finally, we study the influences of the incident angle on the enhanced excitation of the silicon nanowire with the designed head, where the incident angle is the angle between the x-axis and the propagating direction of the incident wave. In this simulation, the silicon nanowire with $w = 100$ nm and $L = 10$ μm connected with a silicon flat-ended head with R $= 1$ μm and S $= 400$ nm under 1550 nm illumination is chosen. And the results are shown in figure 6. Power propagating inside of the silicon nanowire as a function of the incident angle at the 1–1 cross section shown in figure 1 is provided in figure 6(a). The detailed information inside of the red dotted box (shown in figure 5(b)) along x direction at the nanowire center is presented in figure 6(b) for intensity distributions under four kinds of incident waves, while the intensity distribution of incident angle $\alpha = 5°$ is given in figure 6(c). It can be seen that as the incident increases, the power propagating inside of the silicon nanowire decreases. By comparing figures 5(b) and 6(c), the maximum of intensity is reduced less than 10%

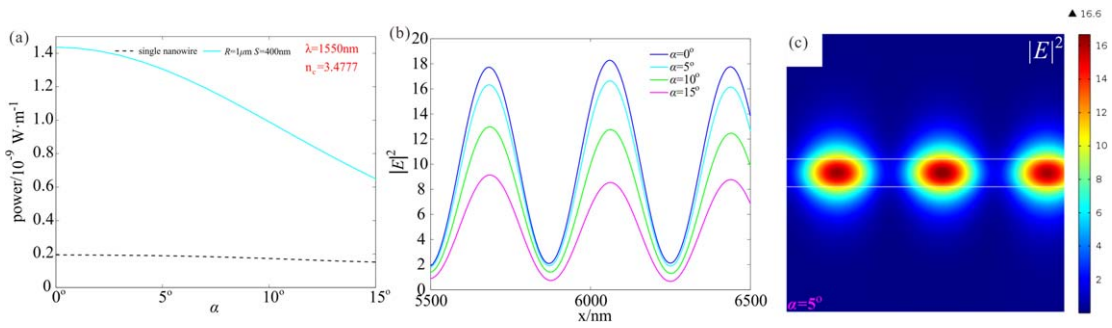

Figure 6. Power propagating inside of the nanowire as a function of the incident angle at the 1–1 cross section shown in (a), while the detailed information inside of the red dotted box (shown in figure 5(b)) along x direction at the nanowire center is presented in (b) for intensity distributions, and the intensity distributions of the incident angle $\alpha = 5^\circ$ is picked out in (c). The other parameters are the same as those in figure 5(b).

when the incident angle increases from 0° into 5°. This indicates that there is a certain stability of the nanowire with a designed flat-ended head for not perfect normal incidence.

4. Conclusion

In conclusion, a method for enhancing the excitation of a high-index nanowire by adding a flat-ended head is demonstrated. With the assistant of the flat-ended head, intensity and power flow of the high-index nanowire under a plane wave can be improved. Our simulation shows that the enhancement factor is influenced by the length and the refractive index of the nanowire, and the size of the flat-ended head. By carefully selecting the size of the flat-ended head, the intensity enhancement factor can reach more than 10 times of that without a head. This method is also effective in the excitation of the silicon nanowire at a near-infrared wavelength illumination and has a certain stability for not perfect normal incidence. Our results provide a way to design the high-index nanowire with high-intensity excitation. This method can also be used for the high excitation of high-index nano-waveguides illuminated under a free space light or a fiber-end-face illumination. Our results may have potential applications for adopting the high-index nanowire realizing on-chip optical sorting and sensoring.

Acknowledgments

This work was supported by the Natural Science Research Program of Huai'an (No. HAB202153), National Natural Science Foundation of China (61974143) and Youth Innovation Promotion Association of the Chinese Academy of Sciences (2020223).

Data availability statement

No new data were created or analysed in this study.

Disclosures

The authors declare no conflicts of interest.

ORCID iDs

Song Zhou https://orcid.org/0000-0003-0358-1309

References

[1] Huang Y, Duan X, Cui Y, Lauhon L J, Kim K-H and Lieber C M 2001 Logic gates and computation from assembled nanowire building blocks *Science* **294** 1313–7
[2] Brönstrup G, Jahr N, Leiterer C, Csáki A, Fritzsche W and Christiansen S 2010 Optical properties of individual silicon nanowires for photonic devices *ACS Nano* **4** 7113–22

[3] Namdari P, Daraee H and Eatemadi A 2016 Recent advances in silicon nanowire biosensors: synthesis methods, properties, and applications *Nanoscale Res. Lett.* **11** 406–406
[4] Irrera A, Artoni P, Saija R, Gucciardi P G, Iatì M A, Borghese F, Denti P, Lacona F, Priolo F and Maragò O M 2011 Size-scaling in optical trapping of silicon nanowires *Nano Lett.* **11** 4879–84
[5] Schmidt B S, Yang A H J, Erickson D and Lipson M 2007 Optofluidic trapping and transport on solid core waveguides within a microfluidic device *Opt. Express* **15** 14322–34
[6] Yang A H J, Moore S D, Schmidt B S, Klug M, Lipson M and Erickson D 2009 Optical manipulation of nanoparticles and biomolecules in sub-wavelength slot waveguides *Nature* **457** 71–5
[7] Xu X, Wang G, Jiao W, Ji W, Jiang M and Zhang X 2018 Multi-level sorting of nanoparticles on multi-step optical waveguide splitter *Opt. Express* **26** 29262–71
[8] Zhao H, Chin L K, Shi Y, Liu P Y, Zhang Y, Cai H, Yap E P H, Ser W and Liu A Q 2021 Continuous optical sorting of nanoscale biomolecules in integrated microfluidic-nanophotonic chips *Sensors and Actuators B-Chemical* **331** 129428
[9] Ren Y, Chen Q, He M, Zhang X, Qi H and Yan Y 2021 Plasmonic optical tweezers for particle manipulation: principles, methods, and applications *ACS Nano* **15** 6105–28
[10] Chen Z, Taflove A and Backman V 2004 Photonic nanojet enhancement of backscattering of light by nanoparticles: a potential novel visible-light ultramicroscopy technique *Opt. Express* **12** 1214–20
[11] Luk'yanchuk B S, Paniagua-Domínguez R, Minin I V, Minin O V and Wang Z 2017 Refractive index less than two: photonic nanojets yesterday, today and tomorrow *Opt. Mater. Express* **7** 1820–47
[12] Zhu J and Goddard L L 2019 All-dielectric concentration of electromagnetic fields at the nanoscale: the role of photonic nanojets *Nanoscale Advances* **1** 4615–43
[13] Darafsheh A 2021 Photonic nanojets and their applications *J. Phys.: Photonics* **3** 22001
[14] Guo H, Han Y, Weng X, Zhao Y, Sui G, Wang Y and Zhuang S 2013 Near-field focusing of the dielectric microsphere with wavelength scale radius *Opt. Express* **21** 2434–43
[15] Zhang Q, Li J, Pan X, Liu X and Gai H 2021 Low-numerical aperture microscope objective boosted by liquid-immersed dielectric microspheres for quantum dot-based digital immunoassays *Anal. Chem.* **93** 12848–53
[16] Zhen Z, Huang Y, Feng Y, Shen Y and Li Z 2019 An ultranarrow photonic nanojet formed by an engineered two-layer microcylinder of high refractive-index materials *Opt. Express* **27** 9178–88
[17] Pacheco-Peña V and Beruete M 2019 Photonic nanojets with mesoscale high-index dielectric particles *J. Appl. Phys.* **125** 84104
[18] Zhou S and Zhou T 2020 An ultra-narrow photonic nanojet generated from a high refractive-index micro-flat-ended cylinder *Applied Physics Express* **13** 42010
[19] Zhou S and Yu M 2021 Engineering an ultra-narrow localized optical beam with a hybrid flat-ended microcylinder *Opt. Quantum Electron.* **53** 1–9
[20] https://comsol.com/
[21] Palik E D 1998 *Handbook of Optical Constants of Solids* (New York: Academic)